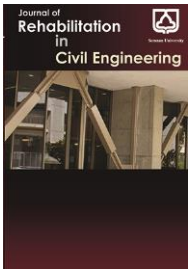

journal homepage: http://civiljournal.semnan.ac.ir/

Simulation of the Reactive Powder Concrete (RPC) Behavior Reinforcing with Resistant Fiber Subjected to Blast Load

H. Akbarzadeh Bengar[1]* and M.R. Yavari[2]
1. Department of Civil Engineering, University of Mazandaran, Babolsar, Iran
2. Department of Flight and Engineering, Imam Ali University, Tehran, Iran

*Corresponding author: h.akbarzadeh@umz.ac.ir

ARTICLE INFO

Article history:
Received: 05 August 2015
Accepted: 15 November 2016

Keywords:
Reactive Powder Concrete (RPC),
Blast load,
Analytical simulation,
Explosion charge,
Explosion point.

ABSTRACT

In research or experimental works related to blast loads, the amount of explosion material and distance of explosion point are very important. So, in this paper has been attempted to present a parametric study of the reactive powder concrete subjected to blast load. The effect of the different amount of TNT adopted the literature, distance of explosion point from RPC slab and also the location of explosion charge (horizontal and vertical coordinates form the center of specimens) has been investigated. In order to the analytical simulation of RPC behavior against blast and also the accuracy of acquired results, at first using ABAQUS software, a RPC slab studied in the literature has been verified. The obtained results are showed that the simulated model of RPC is match with literature one. In the next stage, a case study of the effect of explosion charge and also the distance of explosion point from RPC and NSC (normal strength concrete) slabs have been examined, and the results have been compared. It's noted that the NSC slab is supposed to be a reinforced concrete, whereas 2% volume of special short steel fibers were used in the RPC specimen. The acquired results have been showed that the RPC have better blast explosion resistance than reinforced normal strength concrete.

1. Introduction

In recent years, there have been numerous explosion-related accidents due to military and terrorist activities. To protect structures and save human lives against explosion accidents, better understanding of the explosion effect on structures is needed. In an explosion, the blast load is applied to concrete structures as an impulsive load of extremely short duration with very high pressure and heat. Generally, concrete is known to have a relatively high blast resistance compared to other construction materials. However, normal strength concrete structures require higher strength to improve their resistance against impact and blast loads.

Therefore, a new material with high-energy absorption capacity and high resistance to damage is a better material for blast resistance design. Recently, Ultra High Strength Concrete (UHSC) and Reactive Powder Concrete (RPC) have been actively developed to significantly improve concrete strength [1-2]. Reactive powder concrete (RPC), otherwise known as ultra-high-performance concrete, was developed through microstructural enhancement techniques for cementitious materials. As compared to ordinary cement-based materials, the primary improvements of RPC include the particle size homogeneity, porosity, and microstructures. The mechanical properties that can be achieved include the compressive strength of the range between 200 and 800 MPa, fracture energy of the range between 1200 and 40,000 J/m2, and ultimate tensile strain at the order of 1%. [1-2]. This is generally achieved by microstructural engineering approach, including elimination of the coarse aggregates, reduction of the water-to-cementitious material, lowering of the CaO–SiO2 ratio by introducing the silica components, and incorporation of steel fiber reinforcement [3–5]. The reinforcing effect of steel fibers is especially critical to the mechanical properties of RPC under tension. Among many UHPCs available on the market, ultra-high strength concrete (UHSC) and reactive powder concrete (RPC) are the most widely used [6]. However, because of their ultra-high strengths and manufacturing costs, the use of UHSC and RPC has been questioned, with concerns raised about possible ultra-brittle failure and unfavorable cost-to-performance efficiency. The UHSC specimen had a higher elastic modulus than the RPC specimen for two reasons. Firstly, UHSC has a higher material rigidity than RPC, because UHSC is denser than RPC, and secondly, RPC is more deformable than UHSC, because RPC contains short steel fibers which create multiple interfaces (similar to voids) in the material [7]. RPC is a more appropriate construction material for military facilities and important structures than conventional concrete owing to its enhanced workability and mechanical properties. Reactive powder concrete (RPC) is advanced cement based material, which originally developed in the early 1990s by Bouygues' laboratory in France [8]. RPC possess ultra-high static and dynamic strength, high fracture capacity, low shrinkage and excellent durability under severe condition [5, 8-10].

Jörg Jungwirth(2002) observed that the behavior of RPC in compression is characterized by an initially steady, linear load-deformation relationship, a short nonlinear phase and then fracture, which is associated with a decrease in the stress. The stress then stabilizes at a residual value (Fig. 1). The heat treatment has a considerable influence on the compressive resistance. With curing at 90°C, the compressive resistance rises from 120 MPa to 180 MPa. The failure pattern was characterized by a typical diagonal crack [11].

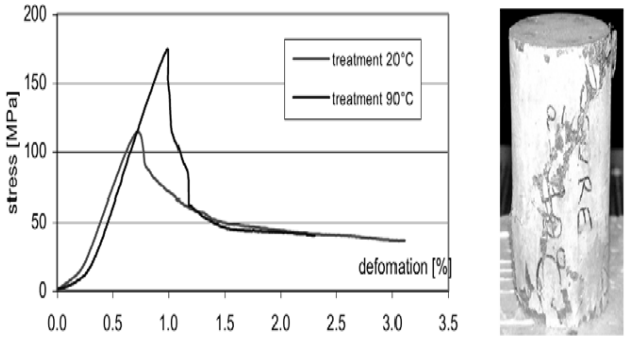

Fig. 1. Stress-strain Curve of RPC and Failure Pattern [11].

Based on a composite material developed by Richard and Cheyrezy (1994, 1995), reactive powder concrete (RPC) is characterized by its material's uniformity that is increased by eliminating coarse aggregate and using silica sand with amaximum particle size of 400 μm. Additionally, concrete density is increased by selecting optimum particle size components [1, 8]. Zanni et al., (1996) observed the working mechanism of RPC's high strength and durability while studying its microstructure. Based on use of nuclear magnetic resonance technology, Zanni et al. (1996) investigated the hydration and pozzolanic reaction inside a specimen that received 20 ◦C and 250 ◦C heat curing. According to their results, the amount of silica fume that participated in hydration was directly proportional to the heat curing temperature [12]. Bayard and Plé (2003) found that the distribution of steel fibers in RPC significantly affects its mechanical behavior. Additionally, the

distribution could be adjusted via a modified casting procedure to enhance its mechanical performance [13]. Chan and Chu (2004) elucidated how silica fume content affects the cohesion between the RPC base material and steel fibers, indicating that cohesive results are optimum when the silica fume contents ranged from 20–30% [14].

The microstructure of RPC is optimized by precise gradation of all particles in the mix to yield maximum compactness. With these merits, RPC has a great potential prospect in the protective shelter of military engineering and nuclear waste treatment, which has received significant concerns from experts across the word [15–17]. However, the high cost, complex fabrication technique and high energy demand of RPC severely limit its commercial development and application in the practical engineering [18,19].

The main purpose of this study is evaluating the blast resistance capacities of NSC (normal strength concrete) and RPC (reactive powder concrete) to determine whether these materials are suitable for use in structures susceptible to terrorist attacks or accidental impacts. In order to, at first for accuracy of acquired results, using ABAQUS software, a RPC slab studied in the literature has been verified. The obtained results are showed that the simulated model of RPC is match with literature one. In resumption, a parametric study having 4 scenarios having different characteristics of NSC and RPC subjected to blast load has been performed. The result show that the robustness of RPC behavior rather than NSC against blast loads. Numerical results demonstrate that the RPC has more resistant than NSC and as an ultra-high strength concrete is suitable for structures under terrorist attacks.

2. Characteristic of blast load

An explosion is a very fast chemical reaction producing transient air pressure waves called blast waves. For a free-air burst, the blast wave will travel away from the source as a spherical wave front as shown in Fig 2(a) ([20-21]). The peak overpressure and the duration of the overpressure vary with distance from the explosives. The magnitude of these parameters also depends on the explosive materials from which the explosive compound is made. Usually the size of the explosive compound is given in terms of a TNT weight. Explosive behavior depends on a number of factors: ambient temperature, ambient pressure, explosive composition, explosive material properties, and the nature of the ignition source type. Additional factors include type, energy, and duration of the events as well as geometry of surroundings (i.e., confined or unconfined). When a condensed high explosive is initiated, explosion reaction generates several additional characteristics such as blast wave of very high pressure, fragmentation from the explosive case or structural elements, hot gas with a pressure from 100 up to 300 kilo bar, and a temperature of about 3,000~4,000℃. The main blast effect is impulsive pressure loading from the blast wave as shown in Fig 2(b) (Baker 1973, Mays & Smith 1995 [22-23]). After a short time, the overpressure behind the shock front drops rapidly and becomes smaller than that of the surrounding atmosphere as shown in Figure 2(b). This pressure domain is known as the negative phase. The front of the blast wave weakens as it progresses outward and its velocity drops toward the velocity of sound in the undisturbed atmosphere. The characteristics of a blast wave resulting from an explosion depend mainly on the physical properties of the source and the medium through which blast waves propagate. To create reference blast experiments, some controlled explosions have been conducted under ideal conditions. To relate other explosions with non-ideal conditions to the reference explosions, blast scaling laws can be employed. The most widely used approach to blast wave scaling is that formulated by Hopkinson, which is commonly described as the cube-root scaling law. The scaled distance, Z, is defined using the Hopkinson-Cranz's cube root law as (ASCE 1999 [24]):

$$Z = R / E^{1/3} \quad or \quad Z = R / W^{1/3} \tag{1}$$

where, Z is scaling distance; R is stand-off distance from the target structure; E is total explosive thermal amount of energy; W is charge weight of equivalent TNT amount. The scaling distance is used for evaluation of blast wave characteristics.

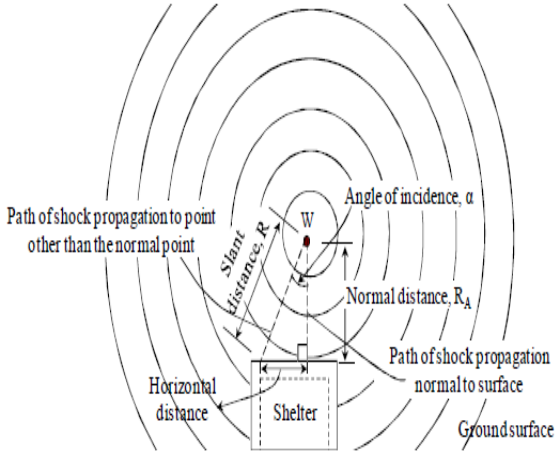

(a) Spherical free air blast

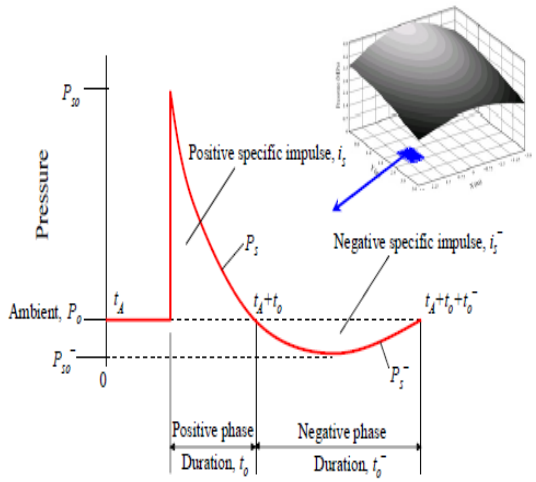

(b) Pressure-time history

Fig. 2. Spherical free air blast ([20-21]).

3. Validation of the simulated model of RPC slab by experimental study

In this part in order to analytical simulation of RPC behavior against blast and also accuracy of acquired results, at first using ABAQUS software, a RPC slab studied in the literature [7] has been verified. The obtained results are showed that the simulated model of RPC is match with literature one with appropriate approximation. A fixed supported rectangular of RPC slab with dimension 1000mm×1000mm ×150mm is presented in this study. In the first step, a comparison between measurement data and experimental modal data tested by Na-Hyun Yi *et al*. [7] is made to validate the accuracy of the numerical modal data. In the experimental test, the RPC slab including 2% volume of special short steel fibers subjected to 15.88 kg of ANFO and a standoff distance of 1.5 m from the center of the slab was selected for the main test as Fig. 3.

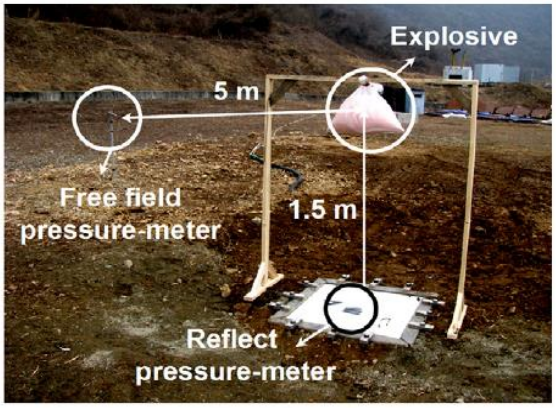

(a)

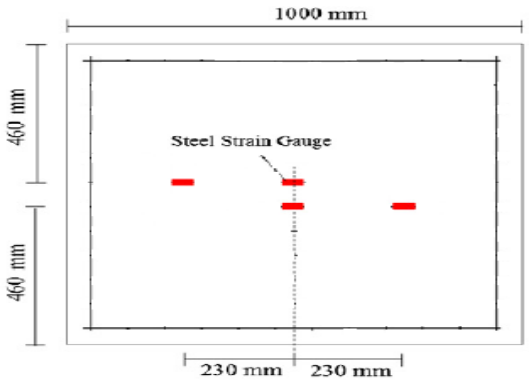

(b)

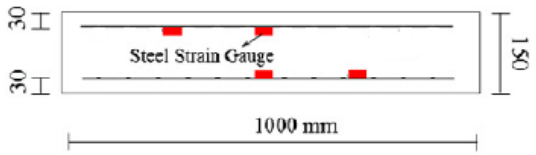

(c)

Fig. 3. Measurement sensor locations: (a) pressure-meter placement setup photo, (b) dimension of the RPC slab (c) cross section of RPC slab [7].

The reflected pressures versus time measurements chart at the center of RPC slab subjected to 15.88 (kg) ANFO and stand-off 1.5 (m) has been showed in Fig. 4. After experimental test, the center displacement of RPC slab versus time chart under blast loading has been presented in Fig.5 and also characteristics of maximum residual displacement measurement from blast loading have been listed in the Table 1.

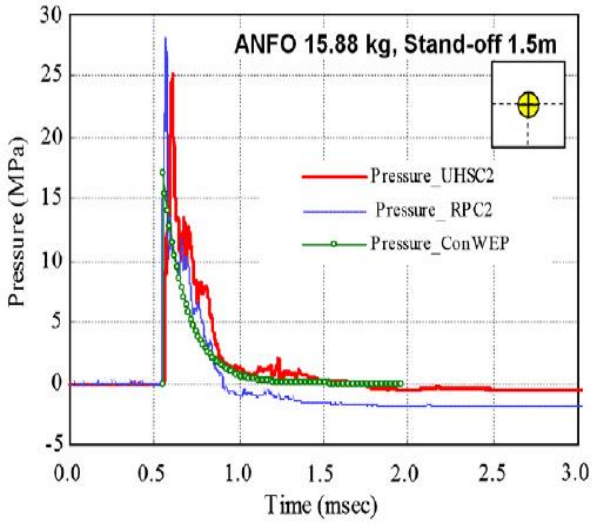

Fig. 4. Reflected pressures versus time measurements of various top surface locations from the main test (15.88 kg ANFO): the center

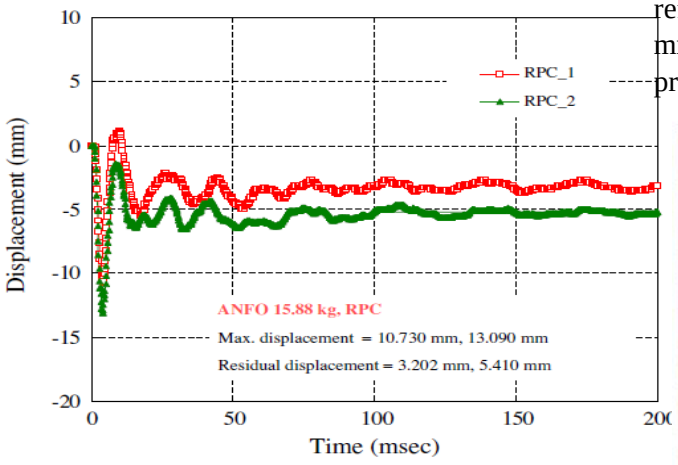

Fig. 5. Center displacement versus time measurements from blast loading: RPC

Table 1. Maximum and residual displacement measurements from blast loading.

Specimen		Experiment results (mm)	
		Max. displacement	Residual displacement
RPC	Case 1	10.73	3.20
	Case 2	13.09	5.41

As can be observed in the Fig. 4, 5 and Table 1, the maximum pressure of RPC specimen, maximum displacement and residual displacement are 28 (MPa), 13.09 (mm) and 5.241 (mm), respectively. In order to verify of the experimental model, the ABAQUS software v 6.12.1 has been used. The model consists of two members: concrete slab and metal support, which is visible in the figures below (Figs. 6, 7(a) and 7(b)). Metal frame support has been defined as elastic. For simulation of concrete behavior, damaged concrete plasticity model has been used. The compressive strengths, the elastic modulus of sampled specimen and the average tensile strengths of experimental RPC slab are 202 MPa, 50.7 GPa, 21.4 MPa, respectively. The starting point of explosion has been placed at a distance of 1.5 (m) above center of RPC slab. For blast simulation, canopy formulation has been used. For simulation of support situation, 4 edge of frame has been supposed to be fixed. The model and mesh of simulated RPC slab is visible in the Figs. 8 (a), (b). The fiber's characteristics have been cited in the literature. As mentioned in the referenced paper the fiber has a length about 13 mm and the stress-strain curve has been presented in Fig. 9.

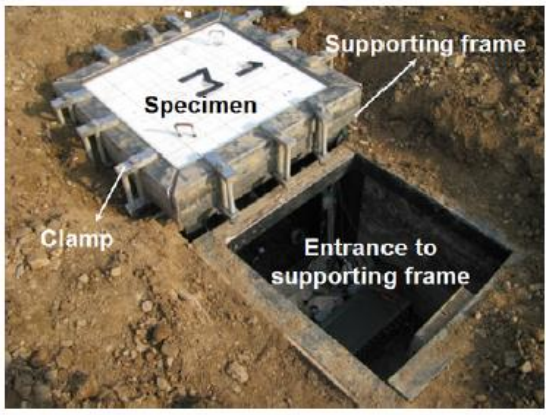

Fig. 6. Photo of the buried supporting frame setup.

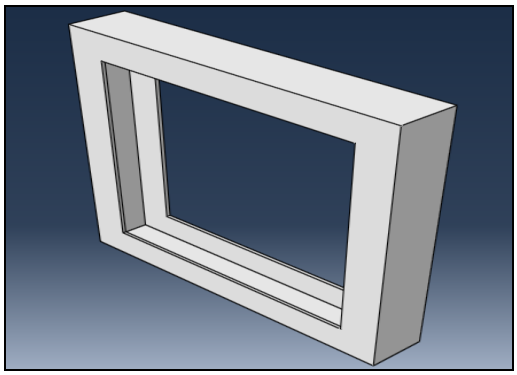

(a)

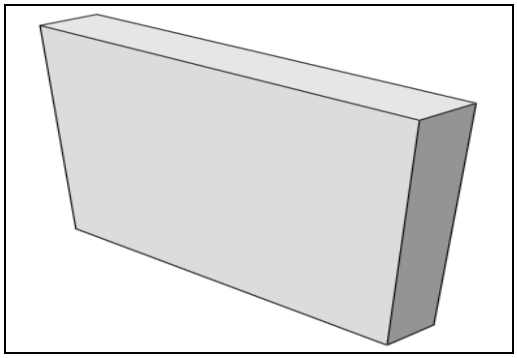

(b)

Fig. 7. Photo of the simulated models in ABAQUS: (a) metal frame support (b) RPC slab.

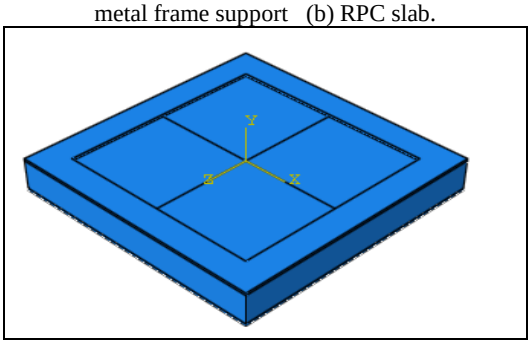

(a)

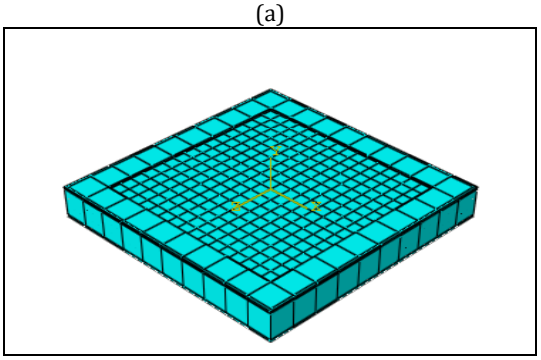

(b)

Fig. 8. Photo of the simulated models in ABAQUS: (a) model of RPC slab (b) mesh of RPC slab.

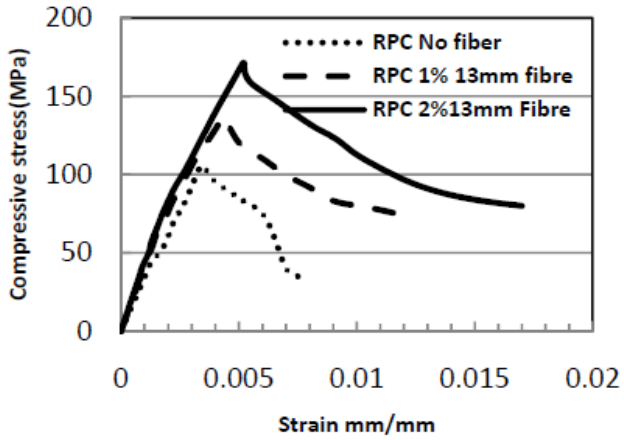

Fig. 9. The compressive stress-strain curve having fiber about 13 mm of length [25]

After modeling of RPC slab, a nonlinear dynamic analysis has been performed on simulated model. Then the pressure-time and displacement-time charts from the center of RPC slab have been extracted. As can be observed in the charts (Fig. 12), the maximum displacement and residual displacement of RPC slab are 9 (mm) and 3.22 (mm), respectively. Also according acquired results, the maximum error rate of displacement is about 15 % and error rate of residual of displacement is less than 1%. These results indicated that reflected displacement is highly dependent on experimental variabilities and environmental conditions, validating the implementation of a magnification factor in the ConWEP calculation [26, 27]. The experimental data were inconsistent due to experimental variations and environmental conditions (i.e., charge shape, charge angle, wind velocity, humidity, etc.). However, the overall blast pressure data agreed well with the ConWEP results.

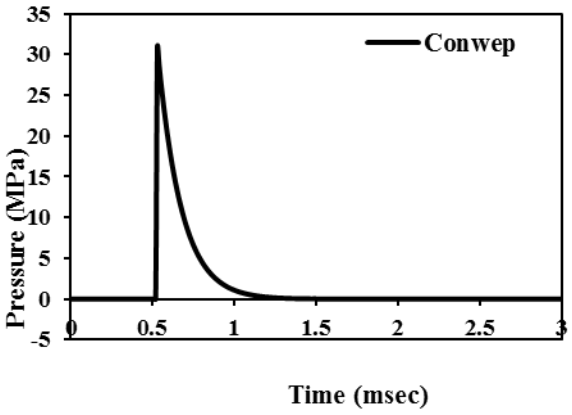

Fig. 10. The pressure-time chart of simulated RPC slab.

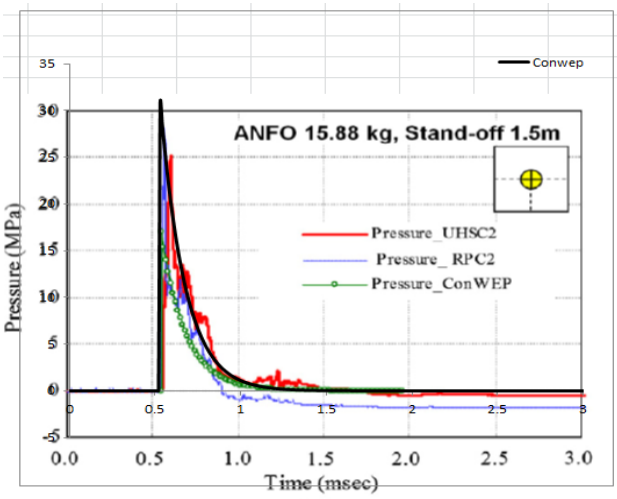

Fig. 11. Comparison of the pressure-time charts of experimental and simulated (black) RPC slab.

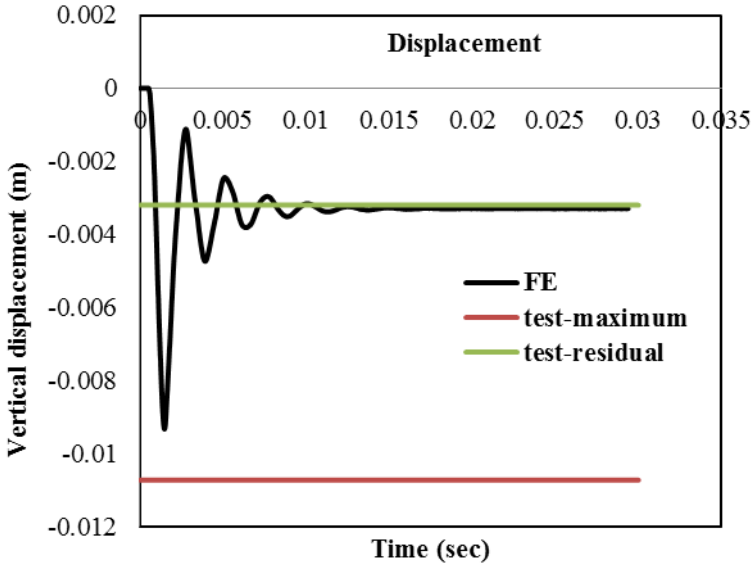

Fig. 12. The displacement-time chart of simulated RPC slab: (a) the FE simulation (black) (b): the maximum displacement of experimental result (red) (c): the residual displacement of experimental result (green)

After nonlinear analysis the displacement contour, main stress and plastic strain of simulated RPC slab has been extracted from ABAQUS software (Figs. 13-15).

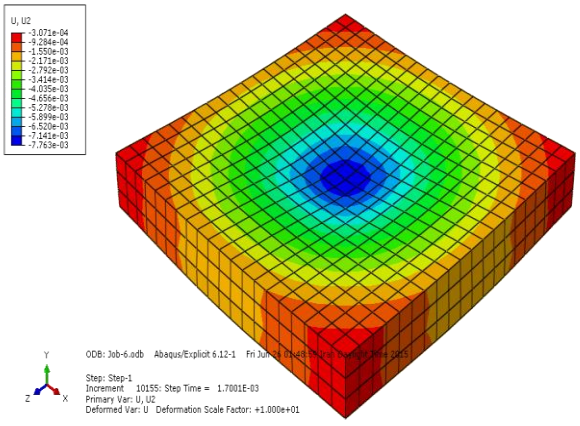

Fig. 13. The displacement contour of the simulated models in ABAQUS at 1.7 (msec) after explosion

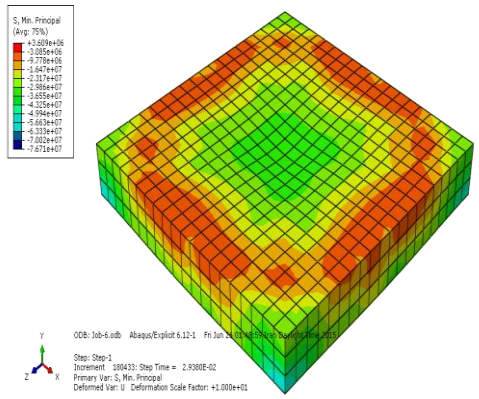

Fig. 14. The main stress contour of the simulated models in ABAQUS at 30 (msec) after explosion

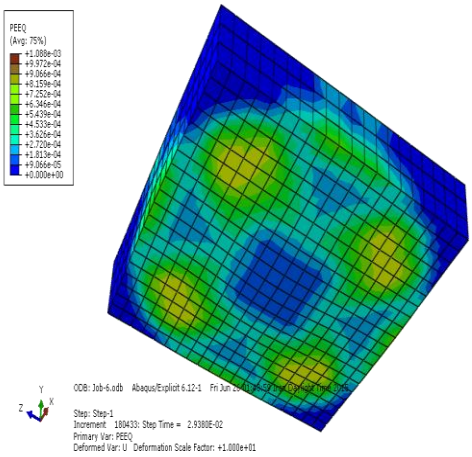

Fig. 15. The equivalent plastic strain contour of the simulated models in ABAQUS at 30 (msec) after explosion

4. Numerical examples

In order to assess the efficiency of the RPC slab subjected to blast load versus NSC, a test example including 4 scenarios have been listed in Table 3. Two main parameters consist of explosion charge and explosion point has been considered. In order to simulate an actual blast, for explosion charge, a bomb named Mark 84 General Purpose (GP) Bomb or BLU-117 has been selected here. The characteristic of the bomb is mentioned in section 4.1.

4.1. Characteristic of the Mark 84 bomb

The Mark 84 or BLU-117 is an American general-purpose bomb, it is also the largest of the Mark 80 series of weapons. Entering service during the Vietnam War, it became a commonly used US heavy unguided bomb (due to the amount of high-explosive content packed inside) to be dropped. The Mark 84 has a nominal weight of 2,000 lb (907.2 kg), but its actual weight varies depending on its fin, fuze options, and retardation configuration, from 1,972 to 2,083 lb (894.5 to 944.8 kg). It is a streamlined steel casing filled with 945 lb (428.6 kg) of Tritonal high explosive. The Mark 84 is capable of forming a crater 50 feet (15.2 m) wide and 36 ft (11.0 m) deep. It can penetrate up to 15 inches (381.0 mm) of metal or 11 ft (3.4 m) of concrete, depending on the height from which it is dropped, and causes lethal fragmentation to a radius of 400 yards (365.8 m). The characteristics of MK 84 bomb has been presented in Fig. 16, briefly [27-28].

Mark 84 General Purpose (GP) Bomb

A Mk 84 GP bomb

Type	Low-drag general purpose bomb
Place of origin	United States
Production history	
Unit cost	$3,100[1]
Specifications	
Weight	2039 lb (925 kg)
Length	129 in (3280 mm)
Diameter	18 in (458 mm)
Filling	Tritonal, Minol or Composition H6
Filling weight	945 lb (429 kg)

Fig. 16. Characteristic of the Mark 84 bomb [28-29]

4.2. The results of simulated RPC and NSC slabs subjected to MK 84 bomb

4.2.1 Simulating explosion point at a distance above the center of the specimens

A fixed slab with dimensions 1*1*0.15 (m) shown in Figure 8 is selected as the numerical example for RPC and NSC specimens. The characteristics of analytical models for NSC and RPC specimens have been listed in Table 2. As shown in Table 3, for assessment of the RPC Slab, forth different scenarios have been considered. In these scenarios, the starting point of explosion has been placed at a distance above the center of the specimens as Table 3. It's noted that the explosion charge has been supposed to be equal with 925 kg TNT as a nominal weight of Mark 84 bomb.

Table 2. The characteristics of analytical models(i.e. compressive strength, ….)

Specimens	Elastic modulus (GPa)	Compressive strength (MPa)	Tensile strength (MPa)
NSC	25.74	30	2.40
RPC	50.70	202	21.40

Table 3. A parametric study based on explosion point under Mark 84 bomb

Explosion charge (kg, TNT)	Explosion point (above the center of the RPC slab) (m)
925 (Mark 84 bomb)	4
925 (Mark 84 bomb)	10
925 (Mark 84 bomb)	20
925 (Mark 84 bomb)	30

The identification charts of analytical simulations for scenarios 1-4 have been shown in Figure 17 - 24. The figures consist of pressure-time, vertical displacement and comparison charts for RPC and NSC specimens.

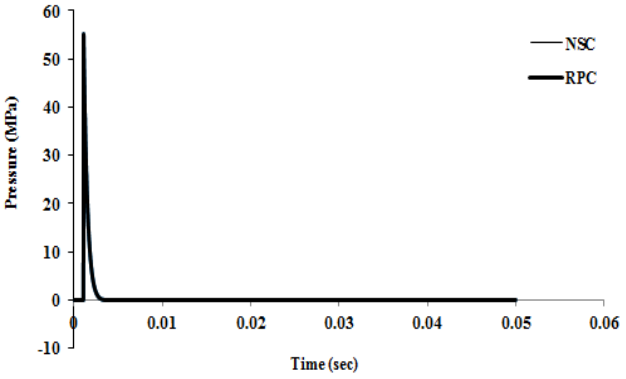

Fig. 17. The pressure-time identification charts for RPC and NSC slabs at a distance 4(m) above the center of the specimens subjected to MK 84 bomb

The Fig. 17 presents explosion pressure due to MK 84 bomb versus time measurement (MPa-sec). As shown in the Fig. 17, the RPC and NSC slabs experience a same pressure of explosion charge at a distance 4 (m) above the center of the specimens. The maximum pressure is 55 (MPa) and occurs at 0.00109 (sec) after starting of explosion.

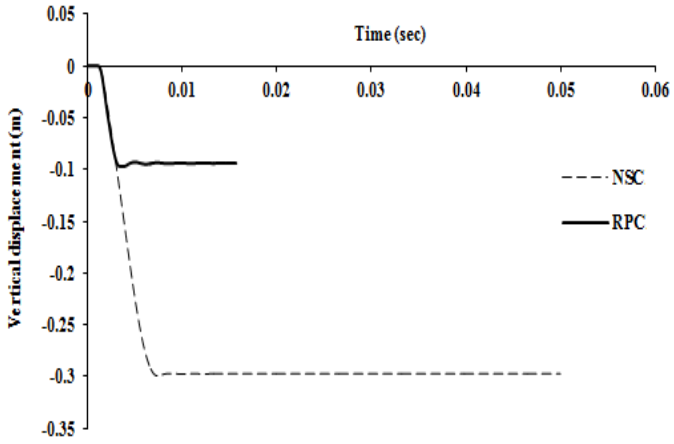

Fig. 18. The displacement-time identification charts for RPC and NSC slabs at a distance 4 (m) above the center of the specimens subjected to MK 84 bomb

The Fig.18 shows that the vertical displacement of NSC and RPC simulated slabs versus time measurements has been compared at a distance 4 (m) above the center of the slabs. The result shows that the RPC slab has a vertical displacement less than NSC one. The maximum vertical displacement of NSC and RPC slab is -

0.2994 (m) and -0.09719 (m), respectively. Also these displacements are experienced at 0.00738 (sec) and 0.0036 (sec) after starting of explosion, respectively. Moreover, the residual displacement of NSC and RPC slabs are -0.2973 (m) and -0.094 (m), respectively. The comparison results of NSC and RPC specimens have been presented in the Table 4, briefly.

Table 4. Comparison of the NSC and RPC results based on explosion point under Mark 84 bomb (scenario 1)

Specimen	NSC slab	RPC slab	The percent of displacement reduction for RPC slab versus NSC one
Maximum displacement (m)	-0.2994	-0.09719	67.54 %
Residual displacement (m)	-0.2973	-0.094	69.36 %

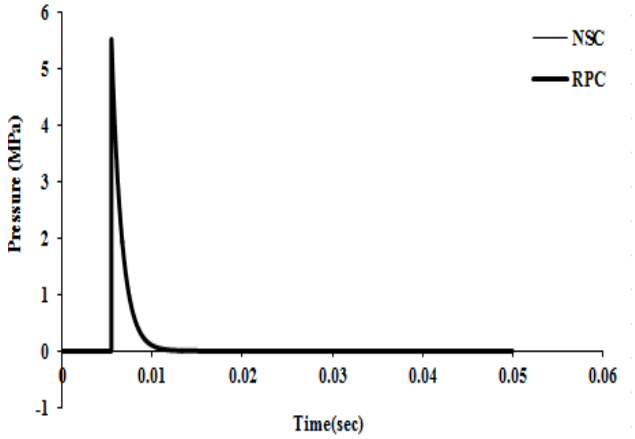

Fig. 19. The pressure-time identification charts for RPC and NSC slabs at a distance 10 (m) above the center of the specimens subjected to MK 84 bomb

The Fig. 19 presents explosion pressure due to MK 84 bomb versus time measurement (MPa-sec). As shown in the Fig. 19, the RPC and NSC slabs experience a same pressure of explosion charge at a distance 10 (m) above the center of the specimens. The maximum pressure is 5.53 (MPa) and occurs at 0.00545 (sec) after starting of explosion.

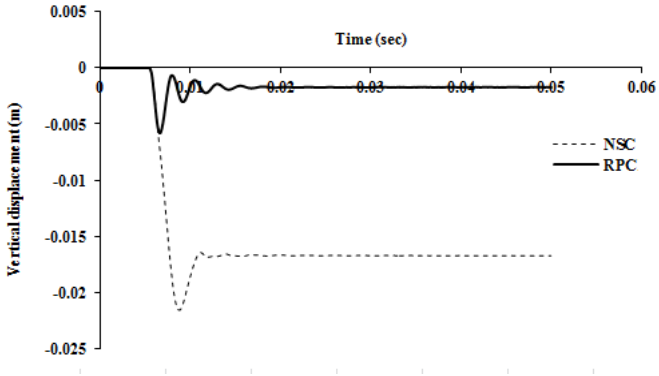

Fig. 20. The displacement-time identification charts for RPC and NSC slabs at a distance 10 (m) above the center of the specimens subjected to MK 84 bomb

The Fig.20 shows that the vertical displacement of NSC and RPC simulated slabs versus time measurements has been compared at a distance 10 (m) above the center of the slabs. The result shows that the RPC slab has a vertical displacement less than NSC one. The maximum vertical displacement of NSC and RPC slab is -0.0216 (m) and -0.0058 (m), respectively. Also these displacements are experienced at 0.0088 (sec) and 0.00662 (sec) after starting of explosion, respectively. Moreover, the residual displacement of NSC and RPC slabs are -0.0167 (m) and -0.0017 (m), respectively. The comparison results of NSC and RPC specimens have been presented in the Table 5, briefly.

Table 5. Comparison of the NSC and RPC results based on explosion point under Mark 84 bomb (scenario 2)

Specimen	NSC slab	RPC slab	The percent of displacement reduction for RPC slab versus NSC one
Maximum displacement (m)	-0.0216	-0.0058	73.15 %
Residual displacement (m)	-0.0167	-0.0017	89.82 %

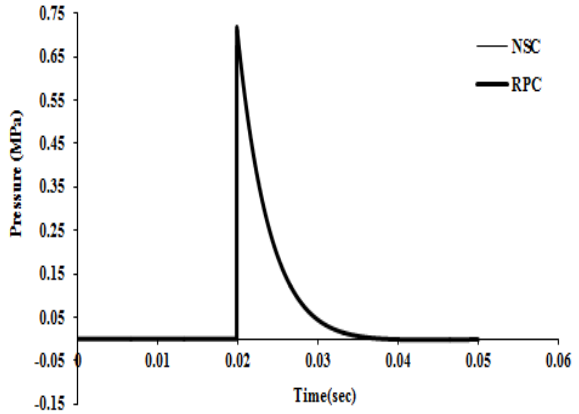

Fig. 21. The pressure-time identification charts for RPC and NSC slabs at a distance 20 (m) above the center of the specimens subjected to MK 84 bomb

The Fig. 21 presents explosion pressure due to MK 84 bomb versus time measurement (MPa-sec). As shown in the Fig. 21, the RPC and NSC slabs experience a same pressure of explosion charge at a distance 20 (m) above the center of the specimens. The maximum pressure is 0.7187 (MPa) and occurs at 0.0199 (sec) after starting of explosion.

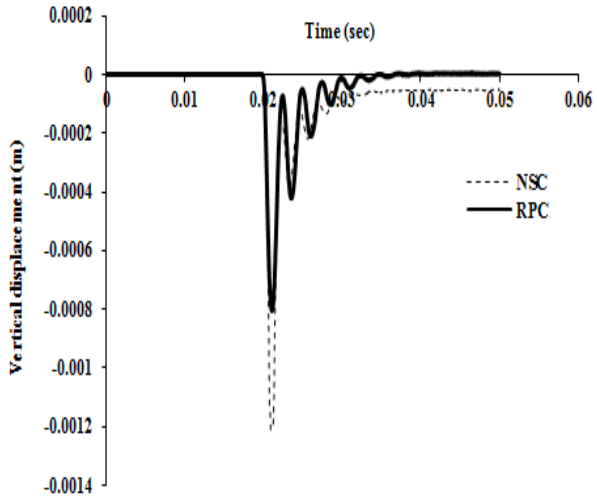

Fig. 22. The displacement-time identification charts for RPC and NSC slabs at a distance 20 (m) above the center of the specimens subjected to MK 84 bomb

The Fig. 22 shows that the vertical displacement of NSC and RPC simulated slabs versus time measurements has been compared at a distance 20 (m) above the center of the slabs. The result shows that the RPC slab has a vertical displacement less than NSC one. The maximum vertical displacement of NSC and RPC slab is -0.00121 (m) and -0.0008 (m), respectively. Also these displacements are experienced at 0.021 (sec) and 0.021 (sec) after starting of explosion, respectively. Moreover, the residual displacement of NSC and RPC slabs are -5.2e-5 (m) and 2.2e-6 (m), respectively. The comparison results of NSC and RPC specimens have been presented in the Table 6, briefly.

Table 6. Comparison of the NSC and RPC results based on explosion point under Mark 84 bomb (scenario 3)

Specimen	NSC slab	RPC slab	The percent of displacement reduction for RPC slab versus NSC one
Maximum displacement (m)	-0.00121	-0.0008	24.79 %
Residual displacement (m)	-5.2e-5	2.2e-6	69.36 %

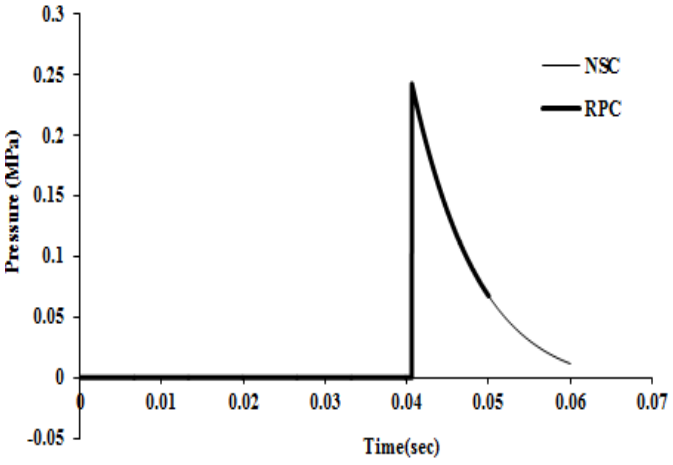

Fig. 23. The pressure-time identification charts for RPC and NSC slabs at a distance 30 (m) above the center of the specimens subjected to MK 84 bomb

The Fig. 23 presents explosion pressure due to MK 84 bomb versus time measurement (MPa-

sec). As shown in the Fig. 23, the RPC and NSC slabs experience a same pressure of explosion charge at a distance 30 (m) above the center of the specimens, approximately. The maximum pressure is 0.242483 (MPa) and occurs at 0.04061 (sec) after starting of explosion.

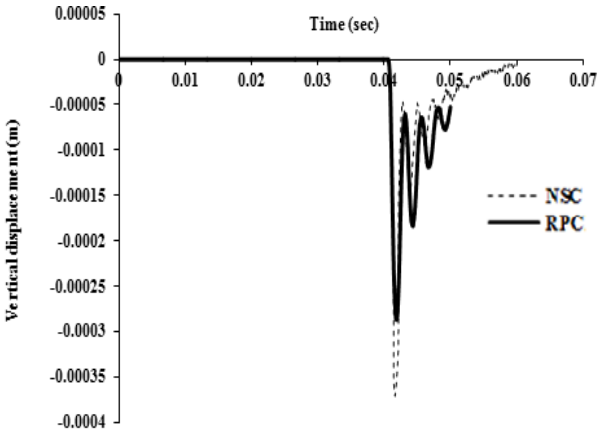

Fig. 24. The displacement-time identification charts for RPC and NSC slabs at a distance 30 (m) above the center of the specimens subjected to MK 84 bomb

The Fig. 24 shows that the vertical displacement of NSC and RPC simulated slabs versus time measurements has been compared at a distance 30 (m) above the center of the slabs. The result shows that the RPC slab has a vertical displacement less than NSC one. The maximum vertical displacement of NSC and RPC slab is -0.00037 (m) and -0.00029 (m), respectively. Also these displacements are experienced at 0.0417 (sec) and 0.0419 (sec) after starting of explosion, respectively.

4.2.2 Simulating explosion point at a horizontal distance from the center of the specimens

In this example a fixed slab with characteristics described in the section 4.2.1 has been selected. As shown in Table 7, for assessment of the robustness of RPC Slab, a different scenario has been considered. In this scenario, the starting point of explosion has been placed at a horizontal distance from the center of the specimens as Table 7. It's noted that the explosion charge has been supposed to be equal with 925 kg TNT as a nominal weight of Mark 84 bomb.

Table 7. A parametric study based on explosion point under Mark 84 bomb

Explosion charge (kg, TNT)	Explosion point (a horizontal distance from the center of the RPC slab) (m)
925 (Mark 84 bomb)	4

The identification charts of analytical simulations for the mentioned scenario have been shown in Figures 25-26. The figures consist of comparison charts of pressure-time and vertical displacement for RPC and NSC specimens.

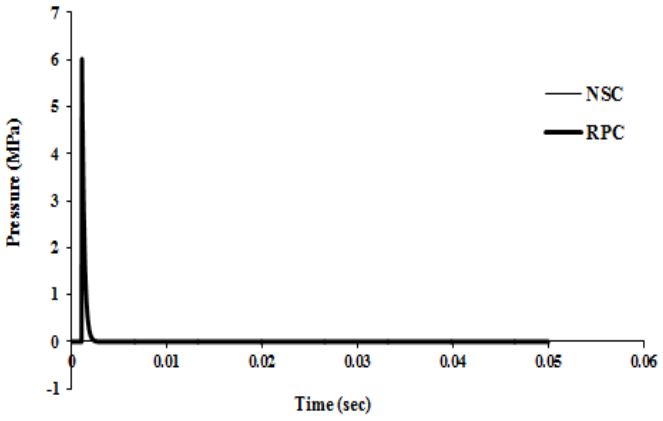

Fig. 25. The pressure-time identification charts for RPC and NSC slabs at a horizontal distance 4 (m) from the center of the specimens subjected to MK 84 bomb

The Fig. 25 presents explosion pressure due to MK 84 bomb versus time measurement (MPa-sec). As shown in the Fig. 25, the RPC and NSC slabs experience a same pressure of explosion charge at a horizontal distance 4 (m) from the center of the specimens. The maximum pressure is 5.985 (MPa) and occurs at 0.00111 (sec) after starting of explosion.

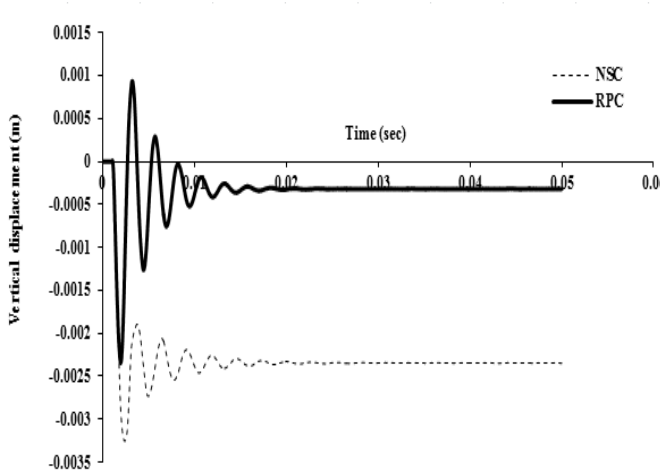

Fig. 26. The displacement-time identification charts for RPC and NSC slabs at a horizontal distance 4 (m) from the center of the specimens subjected to MK 84 bomb

The Fig.26 shows that the vertical displacement of NSC and RPC simulated slabs versus time measurements has been compared at a horizontal distance 4 (m) from the center of the slabs. The result shows that the RPC slab has a vertical displacement less than NSC one. The maximum vertical displacement of NSC and RPC slab is -0.00326 (m) and -0.00234 (m), respectively. Also these displacements are experienced at 0.00242 (sec) and 0.00195 (sec) after starting of explosion, respectively. Moreover, the residual displacement of NSC and RPC slabs are -0.00234 (m) and -0.000321 (m), respectively. The comparison results of NSC and RPC specimens have been presented in the Table 8, briefly.

Table 8. Comparison of the NSC and RPC results based on explosion point under Mark 84 bomb

Specimen	NSC slab	RPC slab	The percent of displacement reduction for RPC slab versus NSC one
Maximum displacement (m)	-0.00326	-0.00234	28.22 %
Residual displacement (m)	-0.00234	-0.000321	86.28 %

5. Conclusion

As a result, as can be observed in the identification charts, in a same pressure, the maximum vertical displacement and also the residual displacement for center of the RPC specimens in all scenarios are less than NSC ones. It's worth nothing that, comparison between the starting point of explosion at horizontal and vertical distances depict that the specimens experience more pressure and vertical displacement when explosion charge has been placed above the center of the slabs than horizontal distance scenario. To this end, it's understood that the RPC slab has more resistant than NSC one and as an ultra-high strength concrete is more suitable for structures under terrorist attacks. Also it's noted that in low distances, the RPC slab has a better behavior rather than NSC one. In other word, the RPC slab is stronger than NSC one and it has a better reaction exposed to MK 84 bomb. Generally, it can be concluded that the RPC have better blast explosion resistance than normal strength concrete.

References

[1] Richard, P., Cheyrezy, M. (1995). "Composition of reactive powder concretes." *Cement and Concrete Research*, Vol. **25** (7), pp. 1501–1511.

[2] Reda, M.M., Shrive, N.G., Gillott, J.E. (1999). "Microstructural investigation of innovative UHPC." *Cem. Concr. Res*. Vol. **29**, pp. 323– 329.

[3] Bonneau, O., Vernet, C., Moranville, M., Aitcin, P.C. (2000). "Characterization of the granular packing and percolation threshold of reactive powder concrete". *Cem. Concr. Res*. Vol. **30**, pp. 1861– 1867.

[4] Feylessoufi, A., Tenoudji, F.C., Morin, V., Richard, P. (2001). "Early ages shrinkage mechanisms of ultra-high performance cement-based materials." *Cem. Concr. Res*. Vol. **31**, pp. 1573– 1579.

[5] Matte, V., Moranville, M. (1999). "Durability of reactive powder composites: influence of silica fume on the leaching properties of

very low water/binder pastes." *Cem. Concr. Compos.* Vol. **21**, pp.1 –9.

[6] Almansour, H., Lounis, Z. (2010). "Innovative design approach of precast-prestressed girder bridges using ultra high performance concrete." *Can J Civil Eng*, Vol.**37**(4), pp.511–21.

[7] Na-Hyun, Yi., Jang-Ho, Jay Kim., Tong-Seok, Han, Yun-Gu, Cho, Jang Hwa, Lee, Blast-resistant characteristics of ultra-high strength concrete and reactive powder concrete (2012). *Construction and Building Materials*, Vol. **28**, pp.694–707.

[8] Richard, P., Cheyrezy, M. (1994). "Reactive powder concretes with high ductility and 200–800MPa compressive strength". In: Proceedings of V.M. Malhotra Symposium "Concrete Technology. Past, Present and Future" ACI SP 144, P.K. Metha, S. Francisco, pp.507–518.

[9] Bonneau, O., Lachemi, M., Dallaire, E. (1997). "Mechanical properties and durability of two industrial reactive powder concretes." *ACI Mater J*, Vol. **94**(4), pp.286–90.

[10] Allan, CLW., Paul, AC., Richard, B. (2007). "Simultaneous measurement of shrinkage and temperature of reactive powder concrete at early-age using fiber Bragg grating sensors." *Cement Concrete Comp*, Vol. **29**(60), pp.490–7.

[11] Jungwirth, J. (2002). "Underspanned Bridge Structures in Reactive Powder Concrete," *4th International Ph.D. Symposium in Civil Engineering*, Munich, Germany.

[12] Zanni, H., Cheyrezy, M., Maret, V., Philippot, S., Nieto, P. (1996). "Investigation of hydration and pozzolanic reaction in reactive powder concrete (RPC) using 29Si NMR". *Cement and Concrete Research*, Vol.**26** (1), pp.93–100.

[13] Bayard, O., Plé, O. (2003). "Fracture mechanics of reactive powder concrete: material modeling and experimental investigations." *Engineering Fracture Mechanics*, Vol.**70** (7–8), pp.839–851.

[14] Chan, Y.W., Chu, S.H. (2004). "Effect of silica fume on steel fiber bond characteristics in reactive powder concrete." *Cement and Concrete Research*, Vol.**34** (7), pp.1167–1172.

[15] Pierre-Claude, A. (2000). "Cements of yesterday and today: concrete of tomorrow." *Cement Concrete Res*, Vol.**30**(9), pp.1349–59.

[16] Cyr, MF., Shah, SP. (2002). "Advances in concrete technology." In: Proceedings of the international conference on advances in building technology, 4–6 December, Hong Kong, China, pp.17–27.

[17] Ming, GL., Yung, CW., Chui, TC. (2007). "A preliminary study of reactive powder concrete as a new repair material. *Constr Build Mater*, Vol.**21**(1), pp.182–9.

[18] Bonneau O., Poulin, C., Dugat, J. (1996). "Reactive powder concretes: from theory to practice." *Concrete Int*, Vol. **18**(4), pp. 47–9.

[19] Cheyrezy M. (1999). "Structural applications of RPC." Concrete, Vol. **33**(1), pp.20–3.

[20] Kim, H.J., Nam, J.W., Kim, S.B., Kim, J.H.J and Byun, K.J. (2007). "Analytical Evaluations of the Retrofit Performances of concrete Wall Structures Subjected to Blast Load." *Journal of the Korea Concrete Institute*, Vol.**19**(2), pp.241-250.

[21] TM5-1300/AFR 88-2/NAVFAC P-39. (1990). "Structures to Resist the Effects of Accidental Explosions." Joint Department of the Army, *Air Force and Navy Washington, DC.*

[22] Baker, W.E. (1973). "Explosion in Air. Wilfred Bker Engineering, San Antonio".

[23] Mays, G.C., and Smith, P.D. (1995). "Blast effect on Buildings: Design of Buildings to Optimize Resistance to Blast Load-ing."

[24] ASCE. (1999). "Structural Design for Physical Security: State of the Practice Report. Task Committee on Physical Security". *American Society of Civil Engineers*, New York.

[25] Lavanya Prabha, S., Dattatreya, J.K., Neelamegam, M. and Seshagiri, RAO M.V. (2010). "Properties of reactive powder concrete under uniaxial compression." Int J Eng Sci Technol, Vol. **2**(11), pp.6408-6416.

[26] Yi, N.H., Kim, S.B., Kim, J.H.J., Cho, Y.G. (2009). "Behavior analysis of concrete structure under blast loading: (II) blast loading response of ultra- high strength concrete and reactive powder concrete slabs (Korean)." *J Korean Soc Civil Eng*, Vol. **29**(5A), pp.565–75.

[27] Nam, JW., Kim, HJ., Kim, SB., Yi, NH., Kim, JHJ. (2010). "Numerical evaluation of the retrofit effectiveness for GFRP retrofitted concrete slab subjected to blast pressure." *Compos Struct*, Vol. **92**(5), pp.1212–22.

[28] https://en.wikipedia.org/wiki/Mark_84_bomb

[29] Don, Holloway. (1996). "STEALTH SECRETS OF THE F-117 NIGHTHAWK: Its development was kept under wraps for 14 years, but by 1991, the F-117 Nighthawk had become a household word. Aviation History (Harrisburg, Pennsylvania: Cowles Magazines)". ISSN 1076-8858.